Stochastic Environmental Research and Risk Assessment

Effect of climate change on the Centennial drought over China using High-Resolution NASA-NEX downscaled climate ensemble

--Manuscript Draft--

Manuscript Number:	SERR-D-18-00203
Full Title:	Effect of climate change on the Centennial drought over China using High-Resolution NASA-NEX downscaled climate ensemble
Article Type:	Original research
Keywords:	Climate change; drought; NASA-NEX; Standardized Precipitation Index; Standardized Precipitation Evapotranspiration Index; China
Abstract:	The impacts of climate change on future drought properties in various regions across the China are accessed using 21 downscaled global climate models provided by NASA (NEX-GDDP) at the Representative Concentration Pathways (RCP) 4.5 and RCP8.5 emission scenarios. And multiple statistical approaches are employed to evaluate the significance of projections. Results show a considerable aggravation in spatial extent and severity of future drought events over the majority of regions, particularly in northwest and northeast China, expect for winter over northeast region. Mild variability of drought extent is projected for Standardized Precipitation Index (SPI). While drought extent for Standardized Precipitation Evapotranspiration Index (SPEI) increases more significantly after the late 2070s under RCP8.5 scenario, and the discrepancies of drought extent are not significant between RCP4.5 and RCP8.5 scenarios in the early and mid-21st century. The increases in drought intensity and frequency are mainly located over north and northwest China in spring, summer and autumn, while shifted into southeast China in winter. Over the northwestern and northern regions of China, dramatic aggravation of drought attribute is projected to the increases in potential evapotranspiration (PET). While the exacerbating drought conditions are expected to the attribution of deficiencies in rainfall in the northwestern region. At national scale, PET plays a more primary role in the future severe and widespread droughts in the context of climate change.

Effect of climate change on the Centennial drought over China using High-Resolution NASA-NEX downscaled climate ensemble

Fuqiang Cao[1] and Tao Gao[2, 3, 4*]

1 School of geosciences, Shanxi Normal University, Linfen 041000, China

2 College of Urban Construction, Heze University, Heze 274000, China

3 State Key Laboratory of Numerical Modeling for Atmospheric Sciences and Geophysical Fluid Dynamics, Institute of Atmospheric Physics, Chinese Academy of Sciences, Beijing 100029, China

[4] Department of Marine, Earth and Atmospheric Sciences, North Carolina State University, Raleigh, North Carolina 27695, USA

Submitted to

Stochastic Environmental Research and Risk Assessment

April 27, 2018

*Corresponding author address: Dr. Tao Gao, 2269 University Road, Heze 274015, P. R. China. Email: tgao.oc@gmail.com

Keywords: Climate change; drought; NASA-NEX; Standardized Precipitation Index; Standardized Precipitation Evapotranspiration Index; China.

Abstract: The impacts of climate change on future drought properties in various regions across the China are accessed using 21 downscaled global climate models provided by NASA (NEX-GDDP) at the Representative Concentration Pathways (RCP) 4.5 and RCP8.5 emission scenarios. And multiple statistical approaches are employed to evaluate the significance of projections. Results show a considerable aggravation in spatial extent and severity of future drought events over the majority of regions, particularly in northwest and northeast China, expect for winter over northeast region. Mild variability of drought extent is projected for Standardized Precipitation Index (SPI). While drought extent for Standardized Precipitation Evapotranspiration Index (SPEI) increases more significantly after the late 2070s under RCP8.5 scenario, and the discrepancies of drought extent are not significant between RCP4.5 and RCP8.5 scenarios in the early and mid-21st century. The increases in drought intensity and frequency are mainly located over north and northwest China in spring, summer and autumn, while shifted into southeast China in winter. Over the northwestern and northern regions of China, dramatic aggravation of drought attribute is projected to the increases in potential evapotranspiration (PET). While the exacerbating drought conditions are expected to the attribution of deficiencies in rainfall in the northwestern region. At national scale, PET plays a more primary role in the future severe and widespread droughts in the context of climate change.

1 Introduction

The Fifth Assessment Report of the Intergovernmental Panel on Climate Change (IPCC AR5) claims that global average near-surface air temperature has increased by approximately 0.78 °C (0.72 to 0.85) since 1900, with much greater trend slope during the last decades (Stocker et al., 2013; Field et al., 2014; Luo and Lau, 2017). The global warming, to a great degree, exacerbates hydrological cycle at multiple scales, these may be compelling to an increase in regional climate extremes, for example, extreme droughts, tropical cyclones and intense precipitation, which results in catastrophic consequence to ecosystem productivity and human survival (Wentz et al., 2007; Trenberth et al., 2014). Drought is recognized as one of the most damaging disasters due to its causes on economic, agriculture and environmental damages (Dai, 2013; Song et al., 2015; Duffy et al., 2015; Zhang and Zhou, 2015). It is therefore of great importance to project further variations in droughts or severe droughts to provide advanced warning for policymakers and stakeholders. Several previous studies focusing on projection of drought variability and impacts have been conducted at global scale (e.g., Cook et al., 2014; Touma et al., 2015), and pointed out that climate change was expected to enhance the drought intensity and frequency by reconciling moisture supply and evaporative demand in the 21st century. Moreover, the droughts are likely to be more intense and set in quicker when they occur under the background of climate change (Trenberth et al., 2014; Huang et al., 2015; Diffenbaugh et al., 2015). Although studying variations in droughts at global scale are beneficial to understand the impacts of climate change on drought variability,

researches conducted at regional and local scales are great crucial to obtain a better understanding of fine-scale drought properties and the possible physical causes as well as a more accurate forecast practice, these may be significantly meaningful to facilitate risk-based planning and provide a framework of adaptive resource management.

Global climate model (GCM) is the principal tool to understand and evaluate the effects of climate change on regional climate extremes whether in the past or the future (Taylor et al., 2012; Wuebbles et al., 2014), since the outputs of GCMs can capture the primary large-scale characteristics and patterns of climatic variables (Sillmann et al., 2013). However, existing studies reported that GCMs overestimates mild precipitation in many regions because of uncertainties in model parameterization, which leads to large biases of raw outputs derived from GCMs (Knutti and Sedláček, 2013; Nasrollahi et al., 2015), and the strong uncertainties still appear in future climate projections that mainly arise from anomalies in both convergence and evapotranspiration (Joetzjer et al., 2013). Sun et al. (2015) showed that raw GCMs from phase 5 of the Coupled Model Intercomparison Project (CMIP5) overestimated the amount of daily precipitation that is less than 5 mm over the entire China, whereas the heavy rainfall with daily precipitation being more than 20 mm tended to be underestimated in humid areas but overestimated over arid regions. In addition, the probabilities of daily mean temperature at lower values were unanimously overestimated over most regions in China, those are generally consistent with projected results based on CMIP5 simulations at global scale (Feng et al., 2014). On

89 the other hand, current GCMs are run at fairly coarse spatial resolutions, and therefore
90 they fail to accurately estimate local meteorological states at scales below 200 km
91 (Meehl et al., 2007; Taylor et al., 2012), and cannot characterize regional drought
92 features required for impact assessment at small scale. van der Wiel et al. (2016)
93 indicated that global coupled climate models improved the ability of reproducing the
94 intensities, spatial patterns and seasonal timing of precipitation over the contiguous
95 United States (CONUS) when the resolution increased from 2° × 2° to 0.25° × 0.25°
96 grid cells. Thus, both the model biases and coarse resolution affect the accuracy of
97 projected regional and local drought changes. Ficklin et al. (2016) investigated the
98 impacts of climate model biases on projections of aridity and drought in the CONUS
99 and demonstrated that considerable enhancements of accuracy of projected droughts
100 were found for bias-corrected and downscaled outputs in comparison with raw GCMs.
101 Furthermore, multiple-model ensemble outperforms individual model in producing
102 projections of meteorological elements, since the multiple-model ensemble may
103 reduce or eliminate effects of uncertainty or biases derived from individual model
104 (Sillmann et al., 2013; Zhou et al., 2014). Therefore, the multi-modeling methods
105 have been receiving increased concerns in projecting drought and wet conditions in
106 numerous regions over the world when utilizing outputs from CMIP5 and other
107 bias-corrected simulated results (e.g., Duffy et al., 2015; Swain and Hayhoe, 2015;
108 Ahmadalipour et al., 2016).

109 China is dominated by different climatic zones on account of its vast territory and
110 complex terrain, and has suffered severe and long-lasting drought disasters during the

last decades. Analyses of observed dataset indicated that droughts have become more frequent and severe over many regions in China (He et al., 2011; Yu et al., 2014; Chen and Sun, 2015; Liu et al., 2016; Gong et al., 2017; Wu et al., 2018). In particular years, the typically regional droughts endured precipitation deficit and abnormal high temperature, leading to severely societal and economic consequences. The once-in-a-century droughts across southwest China, including Guizhou, Yunnan, Sichuan, Guangxi and Chongqing from summer 2009 to spring 2010 and the severe short-term drought in July-August 2013 over southern portion of East China, with air temperature being up to 41-44.5°C in specific regions, were subjected more than 16 million people and 17 million livestock to drinking water shortages (Yang et al., 2012; Sun, 2014). However, the studies on the variations and physical mechanism of droughts in China are mainly concentrated in the analyses of instrumental records, even though some researches were conducted on the projections of future drought changes using outputs of CMIP5 models (e.g., Wang and Chen, 2014), the uncertainties derived from physical parameterized configuration of climate models are hard to be estimated, resulting in the dependence of selection of climate models for the discrepancies of projected patterns and severity of drought conditions (Zhang and Zhou, 2015). Therefore, how the drought is changing across the China in the 21st century under the background of global warming remains unclear, which is the major motivation for us to conduct this work. The primary purpose of this study is to evaluate the influences of climate change on the frequency, intensity and spatial extent of droughts in China using the state-of-the-art downscaling dataset of NASA

Earth Exchange Global Daily Downscaled Projections (NEX-GDDP). It is the first attempt to employ these newly available datasets to assess the impacts of global warming on the future seasonal drought variability over the China. The remainder of this paper is structured as follows. The NEX-GDDP datasets and drought indices as well as methods are described in section 2, and the results are presented in section 3. The relationships between droughts and climate variables are discussed in section 4, followed by summary and conclusions in section 5.

2 Data and methods

2.1 Data

NEX-GDDP datasets are released to access the impacts of global warming at regional and local scales under two representative concentration pathways (RCP4.5 and RCP8.5) (Meinshausen et al., 2011; Thrasher et al., 2013). The Bias-Correction Spatial Disaggregation method is applied to generate these datasets from 21 GCM runs (Table S1) conducted under the CMIP5 (Taylor et al., 2012; Thrasher et al., 2012). Two step process are conducted to deal with outputs of CMIP5 models, the first step is bias correction, which corrects bias of GCMs through comparing with observations. And then all of the 21 model datasets are statistically downscaled to a finer resolution (0.25° × 0.25°, approximately 25 km) by utilizing spatial disaggregation method. Three key climatic variables, including precipitation, maximum and minimum temperature, at daily timescale are available and employed in this study. More information about NEX-GDDP can be obtained via https://nex.nasa.gov/nex/projects/1356/.

155 The observational dataset used in this study is gridded dataset of CN05.1 at daily
156 timescale over the China domain (Wu and Gao, 2013; Wu et al., 2017). The dataset is
157 constructed using "anomaly approach" and first calculated by utilizing thin-plate
158 smoothing splines, then it is derived through angular weighting method. Daily total
159 precipitation, mean, maximum and minimum temperature are available from 1961 to
160 2014 with 0.25° × 0.25° spatial resolution. To better understand drought features over
161 different regions over the China, we divide China into five subregions (Figure 1):
162 northwest China (NW: 35-50°N, 73-105°E), southwest China (SW: 20-35°N,
163 75-105°E), northeast China (NE: 42-55°N, 105-135°E), northern China (NC: 33-42°N,
164 105-135°E), and southeast China (SE: 17-33°N, 105-125°E). These subregions are
165 determined synthetically according to the National Assessment Report on Climate
166 Change (NRC, 2007) and variations in drought conditions of pre-exiting drought
167 studies in China (e.g., Wang and Chen, 2014; Yu et al., 2014; Zhang and Zhou, 2015;
168 Chen and Sun, 2015).

169 *2.2 Drought indices*

170 To facilitate drought monitoring and detection, several objective indices have been
171 proposed in accordance with readily available dataset, for intense, precipitation and
172 temperature (e.g., Palmer, 1965; McKee et al., 1993; Vicente-Serrano et al., 2010),
173 and the important application of appropriate indices to evaluate drought conditions
174 has been also investigated in previous studies (e.g., Mishra and Singh, 2010; Yang et
175 al., 2017). Standardized Precipitation Index (SPI) is adopted by World Meteorological
176 Organization (WMO) and used by hydrological and national meteorological services

177 worldwide to characterize drought variability (Hayes et al., 2011). Nevertheless, SPI
178 solely bases on precipitation variations, without considering other variables that are
179 closely related to droughts such as temperature. Whereas, impacts of temperature are
180 evident for initiating droughts and therefore many studies suggested that large
181 increases in potential evapotranspiration (PET) under a warming climate are also
182 considered as a major factor for drying widespread in addition to precipitation (e.g.,
183 Cook et al., 2014; Scheff and Frierson, 2014). Palmer Drought Severity Index (PDSI)
184 considers the precipitation and temperature simultaneously to identify
185 warming-related drought conditions, while PDSI includes several deficiencies,
186 particularly, the main shortcoming is that it is built-in fixed time scale from 9 to 12
187 months (Wells et al., 2004). Standardized Precipitation Evapotranspiration Index
188 (SPEI) overcomes these limitations of PDSI and also characterizes a multi-temporal
189 phenomenon of droughts as being similar to SPI (Vicente-Serrano et al., 2010; Joshi
190 et al., 2016; Frank et al., 2017). Thus, both SPI and SPEI are employed in the present
191 study because of their applying multi-scale advantages, which is substantial important
192 for assessment of different drought types. And thornthwaite equation (Thornthwaite,
193 1948) is used to evaluate evapotranspiration since many studies have suggested that
194 the technique section does not lead to impacts on SPEI calculation.

195 *2.3 Method*

196 Three major drought features in every season are analyzed for SPEI and SPI,
197 respectively, i. e., spatial extent, intensity and frequency (number of events) of
198 drought. Spatial drought extents are calculated for five divided areas in China.

Long-term trends of the drought intensity are analyzed for the 94-yr period of 2006-2099. And frequency of the drought events is computed for the periods of 2006-2055 and 2050-2099, respectively. Then the variations are investigated by comparing with the frequency of events in the historical period of 1956-2005. In addition, projected drought indices for the future are computed based on the information derived from the historical period. And the basic time period employed to calculate drought indices is 1956-2005, which is consistent with the 50 years for the future two periods. Moreover, the SPEI and SPI are calculated for each of 20 GCMs using 3-month dataset of the precipitation (P) and difference between precipitation and potential evapotranspiration (P-PET). Since the 3-month timescale SPEI and SPI are proved to be the most practical to investigate the seasonal drought variability (Stagge et al., 2015; Ahmadalipour et al., 2017). According to the criteria employed in the previous studies, the values of SPEI and SPI below -1 and -0.8, respectively, are defined as drought onset, representing moderate to extreme drought events (Heinrich and Gobiet, 2012; Chen et al., 2012).

3 Results

3.1 Comparison between observation and downscaled GCMs

The recent research has evaluated the performance and availability of these new statistically downscaled datasets and showed that NEX-GDDP remarkably improved the climate mean precipitation and temperature over China in historical simulation and projections at fine-scale compared to raw CMIP5 models (Bao and Wen, 2017). To examine the ability of NEX-GDDP to reproduce observed geographic distributions

of drought features in China, the comparisons of differences are carried out between precipitation and potential evapotranspiration (P-PET), which are the two crucial factors characterizing variability of droughts, in four seasons (Figure 2). And the period of 1961-2005 for both of downscaled GCMs and CN05.1 is selected to be consistent on the time scale. Figure 2 illustrates that the broad seasonal patterns are similar. In spring, the precipitation is greater than evapotranspiration over southeast coastal areas for both of observed and downscaled datasets, and the opposite situation occurs in northwest China. Subtle discrepancies between them are located over mountainous regions in southwest China, these phenomena are more significant conspicuous for summer, the areas with larger P-PET stretch more widely for observation in southwestern regions of China, even though the spatial distribution of mean P-PET is are generally consistent in summer. In autumn, the few locations with larger observed P-PET appear in middle China, and no significant difference is found in winter. On the whole, the P-PET for NEX-GDDP agree well with observed P-PET derived from these comparisons, implying that downscaled GCMs have robust reliability of future drought projections in China. Thus, the projections of future drought conditions are conducted based on downscaled dataset NEX-GDDP in following sections.

3.2 Spatial extent of drought

The spatial extent of drought, defined by percentage of region with the value of SPEI below -1, is calculated in the five subregions across the China using 21 downscaled GCMs. Drought extent is computed for each year, then mean values and

243 ±1 standard deviation of spatial extent results derived from 21 GCMs are shown in
244 Figure 3.

245 Drought extent is found to be significant increases for each season in all subregions
246 except winter over the NE area, where the barely little variations appear at the end of
247 the 21st century. In particular, NW and NE regions show vast increases in spatial
248 extent of drought in spring, summer and autumn in the distant future. The projected
249 drought extent exhibits largest magnitudes of increases in the NW region, with lower
250 uncertainty compared to NE region, where the extent uncertainty is relatively large
251 excluding winter. The SE region displays relatively small changes in comparison with
252 other subregions, even though this area has more climatological annual rainfall
253 amount. Moderate increases in drought extent are seen in the SW and NC regions,
254 except for the remarkable increases over the SW in spring. Note that drought extent
255 exhibits a slightly increasing trend along with time at the high future emission
256 scenarios (RCP8.5) before around the late 2070s, it is even lower than the growth rate
257 of extent at the intermediate mitigation scenario (RCP4.5), particularly over the NW,
258 NE and NC regions. However, consistently larger projected drought extent occurs by
259 RCP8.5 scenario after the late 2070s until the end of the 21st century. While
260 non-significant variations can be found during this period for RCP4.5 scenario. In
261 addition, there are also similar projected patterns in few seasons at both RCP4.5 and
262 8.5 scenarios, for instance, winter and autumn over the NE and SW regions,
263 respectively. Generally, the downscaled GCMs suggest a relatively increasing spatial
264 extent of projected drought in comparison with historical period. The primary source

of uncertainty in projected drought extent may be the model uncertainty before the late 2070s, after that future scenario uncertainty becomes significant. And great increases in drought extent at the RCP8.5 scenario in later half of the 21st century indicate that high emissions of greenhouse gases induced by human activity have remarkable influences on the future expansion of the arid areas in China.

Corresponding results of drought extent characterized by SPI are illustrated in Figure 4. Visible differences of spatial extent drought appear between SPI and SPEI, since SPI only depends on the variability of precipitation compared to SPEI that reveals the impacts of temperature increases. Figure 4 shows that drought extent for SPI has no remarkable changes over time across the majority of subregions in China, even some appreciable decreases in drought extent at the both emission scenarios are projected over the SW region in summer and autumn.

3.3 Trends of future drought intensity

Figure 5 illustrates the negative trends in the future based on SPEI, which suggests the increasing intensity of drought. Results for RCP4.5 and RCP8.5 are shown in the left and right column, respectively. We only obtain negative trends, intensifying drought conditions, to have a better understanding of drying trends. In order to analyze accurate changes of drought trends, SPEI is computed for each of 21 GCMs and the mean trend is calculated using all 21 downscaled GCMs at every grid cell. Then the average variations of the SPEI per year during the period of 2006-2099 is plotted. It is important to note that a trend of -0.01 in Figure 5 for SPEI indicates that in 50 years (intermediate future) the mean value of the SPEI may decrease by 0.5

(-0.01×50), and also in 94 years (distant future) the mean value of the SPEI may decrease by 1.41 (-0.015×94), which is significant drought conditions with the given thresholds of -1, -1.5 and -2 suggesting moderate, severe and extreme drought conditions, respectively. Therefore, a decrease of -0.5 in SPEI value may worsen the category of drought events by one class.

Trends in future droughts are generally consistent with the regional results of drought extent, with significant increasing droughts over most regions in China in addition to winter. Both of the concentration pathways of RCP4.5 and RCP8.5 exhibit similar spatial patterns of drought trends, while the magnitude of increasing droughts is more severe for RCP8.5, particularly in spring and summer. These suggest that climate change may have a significant impact on future increases in drought intensity across China. For summer, decreasing trends are estimated in most of China except for southwestern regions at both concentration pathways, and severe projected droughts are seen in the north and northwest China, indicating that more intense droughts are expected in summer over these regions. Furthermore, the critical drought conditions are found in western areas of northwest China, where a distinct negative trend of the intensity of drought conditions is detected for all seasons. The spatial pattern of negative trends in autumn is analogous with ones in summer, but with smaller changing magnitude, while no decreasing trends of drought intensity are seen over some regions of southwest China. Note that the spatial distribution of future drought trends in winter is distinguishing compared to other three seasons, with decreasing trends mainly located over central-east and south China, even though

significant negative trends are situated in far western China.

The results of SPI trends are shown in Figure 6. Similar to Figure 5, we only show areas exhibiting decreasing SPI trends, which indicates increasing intensity of drought, to obtain a better understanding of future drying conditions. Unlike the projected changes in SPEI trends, most of China exhibits no negative trends in drought intensity, although exacerbated trends are also found in few subregions for RCP8.5. In autumn, comparing with trend results of SPEI in Figure 5, decreasing trends are located in far western China for both concentration pathways, while this trend pattern is not occurring in other seasons, excepting for RCP8.5 in summer (but no trends for RCP4.5). In winter, the SPI displays a negative trend in southeastern regions of China, where more significant trends are found for the high future emission scenarios (RCP8.5), these are approximately similar to patterns of SPEI trends with major decreasing trends of drought intensity situated over the southeast China.

3.4 Drought frequency

Changes in frequency of projected drought is another meaningful measurement criteria to understand the influence of climate change on future drought over the China in a warming climate. To address this issue, we compare the number of future projected drought events for 50-yr periods to the number of counterpart events during historical period. Future projections of drought events are calculated using the outputs of each downscaled GCM, and the mean frequency from 21 GCMs is considered. Consistent with aforementioned analyses, drought index that is less than or equal to-1 and -0.8 is adopted for SPEI and SPI, respectively, to discern the number of drought

cases. Then the average number of future drought events is compared with those for historical drought events, and the spatial distribution of changes (future minus historical) is demonstrated in 50-yr time frame. These processes are conducted separately at each grid cell in every season. Figure 7 shows the results for SPEI at RCP8.5 emission scenarios during distant future period of 2050-2099. Because there is no spatial change (future minus historical) for SPI and in the intermediate period of 2006-2055 for SPEI, they are omitted to be presented in this study.

The increasing frequency of future drought events is found over the NC and NW regions for RCP8.5 scenario (right panel in Figure 7), particularly in summer and autumn. In spring, the substantial increases in frequency of drought events are mainly located over the Inner Mongolia and portions of Xinjiang. The majority of future frequent droughts situate in the western regions of west China and partial areas over the NC region as well as some intersection areas between NE and NW. The spatial distribution of increasing frequency of future drought events at the RCP8.5 scenario is in accordance with the spatial patterns of larger magnitudes of enhanced drought trends illustrated in the right panel of Figure 5. Little changes of projected drought frequency are seen across eastern and southeastern regions of China, except few areas in winter. For the intermediate mitigation scenario (left panel in Figure 7), the increase in number of projected SPEI drought events principally concentrates over the NW region in summer and autumn. Few locations with increasing drought frequency in spring are found in western regions of China, while there is no change of frequent droughts generated by SPEI at the RCP4.5 scenario in winter. Unlike those for

353 RCP8.5, no strongly similar patterns are found between drought frequency (left panel
354 in Figure 7) and drought trends (left panel in Figure 5) for RCP4.5, even though the
355 trends of future droughts are significant in Figure5.

356 **4 Discussion**

357 The discrepancies of climate are pronounced among different regions across the
358 extensive territory in China. Consequently, the precipitation and temperature
359 anomalies play different roles in detecting droughts over different areas, which is
360 primarily resulting from different climate variability and magnitude of their variability
361 (Chen and Sun, 2015). It is therefore difficult to investigate regional features of
362 projected drought conditions, as the concurrent increase (decrease) of precipitation
363 (temperature) may experience alterations of seasonal climate variables. And the
364 considerable attention may be focusing on the issue about the role of contributions
365 derived from relevant climate variables to future drought variations.

366 Comparisons between SPI and SPEI projected results suggest that it is paramount
367 importance of evapotranspiration induced by increasing temperature for aggravating
368 future drought occurrence. Projected changes in SPI demonstrate that drought extent
369 for SPI has mild variations, while slightly decline is seen in summer and winter over
370 the SW region. Furthermore, little discrepancy is found between two emission
371 scenarios. Changes in drought extent for SPEI is more remarkable compared to SPI.
372 Substantial increases for SPEI are projected in most areas and seasons, only the NE
373 region shows non-significant positive variations in winter. Moreover, the changes in
374 intensity and frequency are more considerable between SPI and SPEI. The majority of

regions, based on SPEI, are expected to experience more aggravated drought events across China, although spatial distribution of trends with increasing drought in winter is different with ones in other seasons. While few areas are expected to be affected by aridity according to SPI.

Both precipitation and PET are employed to calculate SPEI, and changes in any individual climate variable may give rise to variations in SPEI. It is therefore expected that precipitation and PET directly impact the changes in SPEI and temperature may influence the SPEI indirectly, even though temperature is adopted to compute PET as the primary variable. Dramatic escalation of projected drought conditions has be demonstrated in previous analyses, whereas the dominating cause leading to exacerbation of drought conditions is not clear, for instance, increases in seasonal temperature, changes in PET and decreases in rainfall amount. Because the climatic and drying characteristics are different among multiple areas in China, the principal cause may change from region to region. Thus, it is of paramount importance to investigate the relationship and influences of climate variables with aridity at regional scale. To better understand the major causes of variations in future aggravation of drought conditions, variations in seasonality of temperature, PET and precipitation from 21 GCMs are calculated during 50-yr periods of 2006-2055 and 2050-2099, which is in line with the changing periods of SPEI. Because the variations in drought frequency are more significant for RCP8.5 than those of RCP4.5, in this study, spatial correlation analyses for RCP8.5 are conducted using Spearman correlation test in every season to detect the linkages of changes between each variable and drought.

Figure 8 shows the spatial correlation between drought frequency and changes for each variable. Changes in precipitation are negatively correlated with the counterpart of drought, i.e., increasing rainfall will alleviate drying conditions. Changes in PET are positively correlated with drought frequency, i.e., increasing PET would reinforce the drought events.

Different results illustrated in Figure 8 are distinct when assessing the spatial correlation across various regions. For example, over the SW region, changes in PET are highly correlated with variations in drought events in four seasons, especially in summer and autumn. While the correlation of changes between temperature and drought conditions is more significant during intermediate period (2006-2055) in comparison with distant period (2050-2099) for all seasons except autumn. In general, PET plays a crucial role to facilitate the increases in future drought frequency across NW region. In the NE and SE regions, precipitation variations have important impacts on droughts for most of the subregions and seasons except for winter over the NE region. And increases in PET are also the main cause resulting in the enhancement of drought events, in spite of being availability of significant effects from temperature in spring and winter across SE region. On the other hand, less significant spatial correlation between climate variables and projected drought events is found over the SW region compared to those in other subregions. However, drought is closely related to PET and temperature but not for precipitation in this region. The patterns of spatial correlation in the NC region is slightly similar to ones for the NW, and exhibit a high correlation with the amount of PET for summer and autumn. This is associated with

419 drought extent presented in Figure 3, the NW and NC regions show a substantial
420 increase at the RCP8.5 future emission scenario in most seasons.

421 Previous studies focusing on drying spells based on observation in China concluded
422 that drought had become more severe and frequent in China during the past decades,
423 particularly over the NC, NE and NW regions. Moreover, the precipitation and
424 temperature perturbations exhibited different roles in modulating the changes in
425 drought evens (Yu et al., 2014; Chen and Sun, 2015). Two recent works analyzed the
426 drought projection at national scale and claimed that most regions of China were
427 projected to become dryer as a result of increasing PET, and annual drought duration
428 would become longer over the NW region at the RCP8.5 scenario (Wang and Chen,
429 2014; Liang et al., 2017). Nevertheless, both of these studies used outputs of CMIP5
430 and PDSI, which is limited to analyze seasonal variability of future drought
431 conditions. In this study, we investigate the changes in future drought in China by
432 utilizing SPEI, which has advantages in analyzing seasonal aridity. More importantly,
433 we use the state-of-the-art downscaled dataset with high resolution to detect the
434 projections of droughts, and the bias correction has been conducted with observation
435 in comparison with the raw outputs of CMIP5.

436 **5 Summary and conclusions**

437 Effects of climate change on drought conditions will vary in global scope and from
438 location to location, while it is extraordinarily pronounced implications to China.
439 China is vulnerable to climate change on account of its insufficient arable land,
440 confluence of the huge population and economic underdevelopment. It is therefore of

441 particular importance to evaluate the impacts of climate change to future drought
442 variability. In this study, we investigate drought projections across China using 21
443 downscaled CMIP5 GCMs with fine resolution. All the 21 available models are
444 employed during 1961-2099 at both moderate (RCP4.5) and high (RCP8.5)
445 concentration pathways. Space-time characteristics of future drought are analyzed
446 with SPEI and SPI according to seasonal accumulation period.

447 Results show that climate change is expected to reinforce the intensity and spatial
448 extent of drought conditions for most of regions and seasons in China. The projected
449 results show considerable differences between SPEI and SPI, since temperature
450 changes have substantial influences on drought properties, especially in warm seasons
451 (Sherwood and Fu, 2014). Drought extent exhibits mild variations for SPI, while
452 significant increases for SPEI. However, the spatial extent of drought is substantially
453 similar for both RCP4.5 and RCP8.5 before the late 2070s, suggesting that different
454 emission scenarios do not result in significantly different variations in drought area in
455 the early and mid-21st century, while drought extent increases dramatically after
456 2070s over most regions at both emission scenarios, particularly for RCP8.5.
457 Significant increases in frequency and intensity of drought are mainly situated over
458 the NE and NW regions in spring, summer and autumn, except for the SE region in
459 winter. Comprehensive assessment of the major causes contributing to the variability
460 of drought indicate that considerable aggravation of drought attribute is projected to
461 the increases in PET over the NW and NC regions. The NE region exhibits relatively
462 large uncertainty of drought extent coupled with increasing drought intensity in

addition to winter, where the exacerbating drought conditions are expected to precipitation changes. The contributions of changes in precipitation and PET to drought events are less significant over the SW region compared to other regions. In short, regional precipitation deficits and warming conditions collectively characterize changes in future drought events.

Overall, drought is projected to be more frequent and severe in China, especially for RCP8.5 scenario. And the global warming will continue at global scale (Stocker et al., 2013), thus, climate change is going to reinforce considerable effects on the attributes of droughts in the future. Such dramatic increases in droughts driven by climate change would cause substantial influences on agricultural, socioeconomic and hydrological sectors, and also present remarkable adaptation challenges. Our results have meaningful implications for providing useful information to stakeholders to better understand impacts of climate change on regional drought conditions. In addition, changes in onset and duration of future drought, rather than the drought extent and frequency presented in this study are also of great importance requiring further consideration and research.

Acknowledgments

This study is jointly supported by Natural Science Foundation and Sci-tech development project of Shandong Province (No. ZR2018MD014; J15LH10), Project funded by China Postdoctoral Science Foundation (No. 2017T100103; 2016M590127), and the Young Academic Backbone in Heze University (No. XY14BS05). NEX-GDDP dataset is provided by Climate Analytics Group and NASA Ames Research Center using the NASA Earth Exchange.

References

Ahmadalipour, A., Moradkhani, H., and Svoboda, M (2017), Centennial drought outlook over the CONUS using NASA−NEX downscaled climate ensemble, *Int J Climatol*, 37, 2477-2491.

Bao, Y., and Wen, X (2017), Projection of China's near-and long-term climate in a new high-resolution daily downscaled dataset NEX-GDDP, *J*. *Meteor*. *Res*, 31, 236-249.

Chen, G., Tian, H., Zhang, C., Liu, M., Ren, W., Zhu, W., Chappelka, A. H., Prior, S. A., and Lockaby, G. B (2012), Drought in the Southern United States over the 20th century: variability and its impacts on terrestrial ecosystem productivity and carbon storage, *Climatic Change*, 114, 379-397.

Chen, H., and Sun, J (2015), Changes in drought characteristics over China using the standardized precipitation evapotranspiration index, *J Climate*, 28, 5430-5447.

Cook, B. I., Smerdon, J. E., Seager, R., and Coats, S (2014), Global warming and 21st century drying, *Clim Dynam*, 43, 2607-2627.

Dai, A (2013), Increasing drought under global warming in observations and models, *Nature Climate Change*, 3, 52-58.

Diffenbaugh, N. S., Swain, D. L., and Touma, D (2015), Anthropogenic warming has increased drought risk in California, *Proceedings of the National Academy of Sciences*, 112, 3931-3936.

Duffy, P. B., Brando, P., Asner, G. P., and Field, C. B (2015), Projections of future meteorological drought and wet periods in the Amazon, *Proceedings of the National Academy of Sciences*, 112, 13172-13177.

Feng, S., Hu, Q., Huang, W., Ho, C., Li, R., and Tang, Z (2014), Projected climate regime shift under future global warming from multi-model, multi-scenario CMIP5 simulations, *Global Planet Change*, 112, 41-52.

Ficklin, D. L., Abatzoglou, J. T., Robeson, S. M., and Dufficy, A (2016), The influence of climate model biases on projections of aridity and drought, *J Climate*, 29, 1269-1285.

Field, C. B., Barros, V. R., Dokken, D. J., Mach, K. J., Mastrandrea, M. D., Bilir, T. E., Chatterjee, M., Ebi, K. L., Estrada, Y. O., and Genova, R. C.: IPCC, 2014: Climate Change 2014: Impacts, Adaptation, and Vulnerability. Part A: Global and Sectoral Aspects. Contribution of Working Group II to the Fifth Assessment Report of the Intergovernmental Panel on Climate Change., Cambridge

University Press, Cambridge, United Kingdom and New York, NY, USA.

Frank, A., Armenski, T., Gocic, M., Popov, S., Popovic, L., and Trajkovic, S (2017), Influence of mathematical and physical background of drought indices on their complementarity and drought recognition ability, *Atmos Res*, 194, 268-280.

Gong, Z., Zhao, S., and Gu, J (2017), Correlation analysis between vegetation coverage and climate drought conditions in North China during 2001–2013, *Journal of Geographical Sciences*, 27, 143-160.

Hayes, M., Svoboda, M., Wall, N., and Widhalm, M (2011), The Lincoln declaration on drought indices: universal meteorological drought index recommended, *B Am Meteorol Soc*, 92, 485-488.

He, B., Lü, A., Wu, J., Zhao, L., and Liu, M (2011), Drought hazard assessment and spatial characteristics analysis in China, *Journal of Geographical Sciences*, 21, 235-249.

Heinrich, G., and Gobiet, A (2012), The future of dry and wet spells in Europe: a comprehensive study based on the ENSEMBLES regional climate models, *Int J Climatol*, 32, 1951-1970.

Huang, J., Yu, H., Guan, X., Wang, G., and Guo, R (2016), Accelerated dryland expansion under climate change, *Nature Climate Change*, 6, 166-171.

Joetzjer, E., Douville, H., Delire, C., and Ciais, P (2013), Present-day and future Amazonian precipitation in global climate models: CMIP5 versus CMIP3, *Clim Dynam*, 41, 2921-2936.

Joshi, N., Gupta, D., Suryavanshi, S., Adamowski, J., and Madramootoo, C. A (2016), Analysis of trends and dominant periodicities in drought variables in India: A wavelet transform based approach, *Atmos Res*, 182, 200-220.

Knutti, R., and Sedláček, J (2013), Robustness and uncertainties in the new CMIP5 climate model projections, *Nature Climate Change*, 3, 369-373.

Liang, Y., Wang, Y., Yan, X., Liu, W., Jin, S., and Han, M (2017), Projection of drought hazards in China during twenty-first century, *Theor Appl Climatol*. doi: https://doi.org/10.1007/s00704-017-2189-3.

Liu, X., Zhu, X., Pan, Y., Li, S., Liu, Y., and Ma, Y (2016), Agricultural drought monitoring: Progress, challenges, and prospects, *Journal of Geographical Sciences*, 26, 750-767.

Luo, M., and Lau, N (2017), Heat waves in southern China: Synoptic behavior, long-term change, and urbanization effects, *J Climate*, 30, 703-720.

McKee, T. B., Doesken, N. J., and Kleist, J (1993), The relationship of drought frequency and duration

546 to time scales., American Meteorological Society Boston, MA.
547 Meehl, G. A., Stocker, T., Collins, W., Friedlingstein, P., Gaye, A., Gregory, J., Kitoh, A., Knutti, R.,
548 Murphy, J., and Noda, A.: Climate change 2007: The physical science basis, Contribution of
549 working group I to the fourth assessment report of the intergovernmental panel on climate change,
550 747-846.
551 Meinshausen, M., Smith, S. J., Calvin, K., Daniel, J. S., Kainuma, M., Lamarque, J. F., Matsumoto, K.,
552 Montzka, S. A., Raper, S., and Riahi, K (2011), The RCP greenhouse gas concentrations and their
553 extensions from 1765 to 2300, *Climatic Change*, 109, 213.
554 Mishra, A. K., and Singh, V. P (2010), A review of drought concepts, *J Hydrol*, 391, 202-216.
555 Nasrollahi, N., AghaKouchak, A., Cheng, L., Damberg, L., Phillips, T. J., Miao, C., Hsu, K., and
556 Sorooshian, S (2015), How well do CMIP5 climate simulations replicate historical trends and
557 patterns of meteorological droughts? *Water Resour Res*, 51, 2847-2864.
558 National Report Committee, 2007: China's National Assessment Report on Climate Change (in
559 Chinese). Science Press, 148 pp.
560 Palmer, W. C (1965), Meteorological drought, US Department of Commerce, Weather Bureau
561 Washington, DC.
562 Scheff, J., and Frierson, D. M (2014), Scaling potential evapotranspiration with greenhouse warming, *J*
563 *Climate*, 27, 1539-1558.
564 Sherwood, S., and Fu, Q (2014), A drier future? *Science*, 343, 737-739.
565 Sillmann, J., Kharin, V. V., Zhang, X., Zwiers, F. W., and Bronaugh, D (2013), Climate extremes
566 indices in the CMIP5 multimodel ensemble: Part 1. Model evaluation in the present climate, *Journal*
567 *of Geophysical Research: Atmospheres*, 118, 1716-1733.
568 Singh, V. P., Guo, H., and Yu, F. X (1993), Parameter estimation for 3-parameter log-logistic
569 distribution (LLD3) by Pome, *Stochastic Hydrology and Hydraulics*, 7, 163-177.
570 Song, X., Song, S., Sun, W., Mu, X., Wang, S., Li, J., and Li, Y (2015), Recent changes in extreme
571 precipitation and drought over the Songhua River Basin, China, during 1960−2013, *Atmos Res*, 157,
572 137-152.
573 Stagge, J. H., Tallaksen, L. M., Gudmundsson, L., Van Loon, A. F., and Stahl, K (2015), Candidate
574 distributions for climatological drought indices (SPI and SPEI), *Int J Climatol*, 35, 4027-4040.
575 Stocker, T. F., Dahe, Q., Gian-Kasper, P., Tignor, M., Allen, S. K., Boschung, J., Nauels, A., Xia, Y.,

576 Bex, V., and Midgley, P.: Climate Change 2013, The Physical Science Basis. Working Group I
577 Contribution to the Fifth Assessment Report of the Intergovernmental Panel on Climate
578 Change-Abstract for decision-makers.
579 Sun, J (2014), Record-breaking SST over mid-North Atlantic and extreme high temperature over the
580 Jianghuai−Jiangnan region of China in 2013, *Chinese Sci Bull*, 59, 3465-3470.
581 Sun, Q., Miao, C., and Duan, Q (2015), Comparative analysis of CMIP3 and CMIP5 global climate
582 models for simulating the daily mean, maximum, and minimum temperatures and daily precipitation
583 over China, *Journal of Geophysical Research: Atmospheres*, 120, 4806-4824.
584 Swain, S., and Hayhoe, K (2015), CMIP5 projected changes in spring and summer drought and wet
585 conditions over North America, *Clim Dynam*, 44, 2737-2750.
586 Taylor, K. E., Stouffer, R. J., and Meehl, G. A (2012), An overview of CMIP5 and the experiment
587 design, *B Am Meteorol Soc*, 93, 485-498.
588 Thornthwaite, C. W (1948), An approach toward a rational classification of climate, *Geographical*
589 *review*, 38, 55-94.
590 Thrasher, B., Maurer, E. P., McKellar, C., and Duffy, P. B (2012), Technical Note: Bias correcting
591 climate model simulated daily temperature extremes with quantile mapping, *Hydrol Earth Syst Sc*,
592 16, 3309-3314.
593 Thrasher, B., Xiong, J., Wang, W., Melton, F., Michaelis, A., and Nemani, R (2013), Downscaled
594 climate projections suitable for resource management, Eos, Transactions American Geophysical
595 Union, 94, 321-323.
596 Touma, D., Ashfaq, M., Nayak, M. A., Kao, S., and Diffenbaugh, N. S (2015), A multi-model and
597 multi-index evaluation of drought characteristics in the 21st century, *J Hydrol*, 526, 196-207.
598 Trenberth, K. E., Dai, A., Van Der Schrier, G., Jones, P. D., Barichivich, J., Briffa, K. R., and Sheffield,
599 J (2014), Global warming and changes in drought, *Nature Climate Change*, 4, 17-22.
600 van der Wiel, K., Kapnick, S. B., Vecchi, G. A., Cooke, W. F., Delworth, T. L., Jia, L., Murakami, H.,
601 Underwood, S., and Zeng, F (2016), The Resolution Dependence of Contiguous US Precipitation
602 Extremes in Response to CO2 Forcing, *J Climate*, 29, 7991-8012.
603 Vicente-Serrano, S. M., Beguería, S., and López-Moreno, J. I (2010), A multiscalar drought index
604 sensitive to global warming: the standardized precipitation evapotranspiration index, *J Climate*, 23,
605 1696-1718.

606 Wang, L., and Chen, W (2014), A CMIP5 multimodel projection of future temperature, precipitation,
607 and climatological drought in China, *Int J Climatol*, 34, 2059-2078.
608 Wells, N., Goddard, S., and Hayes, M. J (2004), A self-calibrating Palmer drought severity index, *J*
609 *Climate*, 17, 2335-2351.
610 Wentz, F. J., Ricciardulli, L., Hilburn, K., and Mears, C (2007), How much more rain will global
611 warming bring? *Science*, 317, 233-235.
612 Wu, J., Gao, X., Giorgi, F., and Chen, D (2017), Changes of effective temperature and cold/hot days in
613 late decades over China based on a high resolution gridded observation dataset, *Int J Climatol*, 37,
614 788-800.
615 Wu J, Gao X J (2013), A gridded daily observation dataset over China region and comparison with the
616 other datasets. *Chin*. *J*. *Geophys*. 56, 1102–1111, doi: 10.6038/cjg20130406 (in Chinese).
617 Wuebbles, D., Meehl, G., Hayhoe, K., Karl, T. R., Kunkel, K., Santer, B., Wehner, M., Colle, B.,
618 Fischer, E. M., and Fu, R (2014), CMIP5 climate model analyses: climate extremes in the United
619 States, *B Am Meteorol Soc*, 95, 571-583.
620 Wu, J., Miao, C., Tang, X., Duan, Q., and He, X (2018), A nonparametric standardized runoff index for
621 characterizing hydrological drought on the Loess Plateau, China, *Global Planet Change*, 161, 53-65.
622 Yang, J., Gong, D., Wang, W., Hu, M., and Mao, R (2012), Extreme drought event of 2009/2010 over
623 southwestern China, *Meteorol Atmos Phys*, 115, 173-184.
624 Yu, M., Li, Q., Hayes, M. J., Svoboda, M. D., and Heim, R. R (2014), Are droughts becoming more
625 frequent or severe in China based on the standardized precipitation evapotranspiration index: 1951 –
626 2010? *Int J Climatol*, 34, 545-558.
627 Yang, Q., M. Li, Z. Zheng, and Z. Ma (2017) Regional applicability of seven meteorological drought
628 indices in China. *Science China Earth Sciences*, 60, 745-760.
629 Zhang, L., and Zhou, T (2015), Drought over East Asia: a review, *J Climate*, 28, 3375-3399.
630 Zhou, B., Wen, Q. H., Xu, Y., Song, L., and Zhang, X (2014), Projected changes in temperature and
631 precipitation extremes in China by the CMIP5 multimodel ensembles, *J Climate*, 27, 6591-6611.
632

Figures Captions

Fig 1. Five subregions in China. NW: northwest China (35-50°N, 73-105°E), SW: southwest China (20-35°N, 75-105°E), NE: northeast China (42-55°N, 105-135°E), NC: northern China (33-42°N, 105-135°E), and SE: southeast China (17-33°N, 105-125°E).

Fig 2. Comparison of mean precipitation and potential evapotranspiration (P-PET) from 1961-2005 for observation (left panel) and NEX-GDDP (right panel). Black dots indicate significant values at 95% confidence level.

Fig 3. Spatial extent for future drought in the five subregions in China based on 3-month SPEI.

Fig 4. The same as Fig 3. But for SPI.

Fig 5. Long-term trends of drought during the period of 2006-2099 based on 3-month SPEI. Note that a trend with -0.01 for SPEI denotes that in 50 years, the mean value of SPEI will decrease by 0.5 (-0.01×50), this is significant for the given thresholds of -1, -1.5 and -2, which represents moderate, severe and extreme drought, respectively. Black dots indicate that trend significance exceeds the 95% confidence level.

Fig 6. The same as Fig 5. But for SPI.

Fig 7. Changes in the number of drought events based on 3-month SPEI for RCP4.5 (left panel) and RCP8.5 (right panel).

Fig 8. Spatial correlation between the variations in the number of SPEI drought events and changes in the climate variables during the 50-yr future periods for the RCP8.5 scenario.

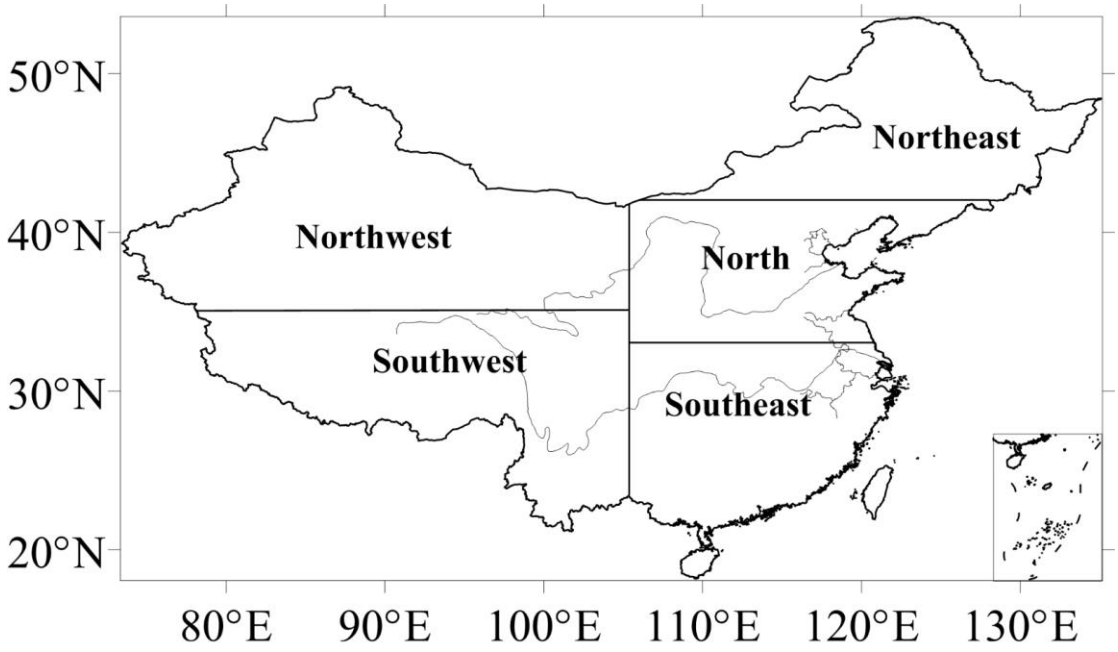

Fig 1. Five subregions in China. NW: northwest China (35-50°N, 73-105°E), SW: southwest China (20-35°N, 75-105°E), NE: northeast China (42-55°N, 105-135°E), NC: northern China (33-42°N, 105-135°E), and SE: southeast China (17-33°N, 105-125°E).

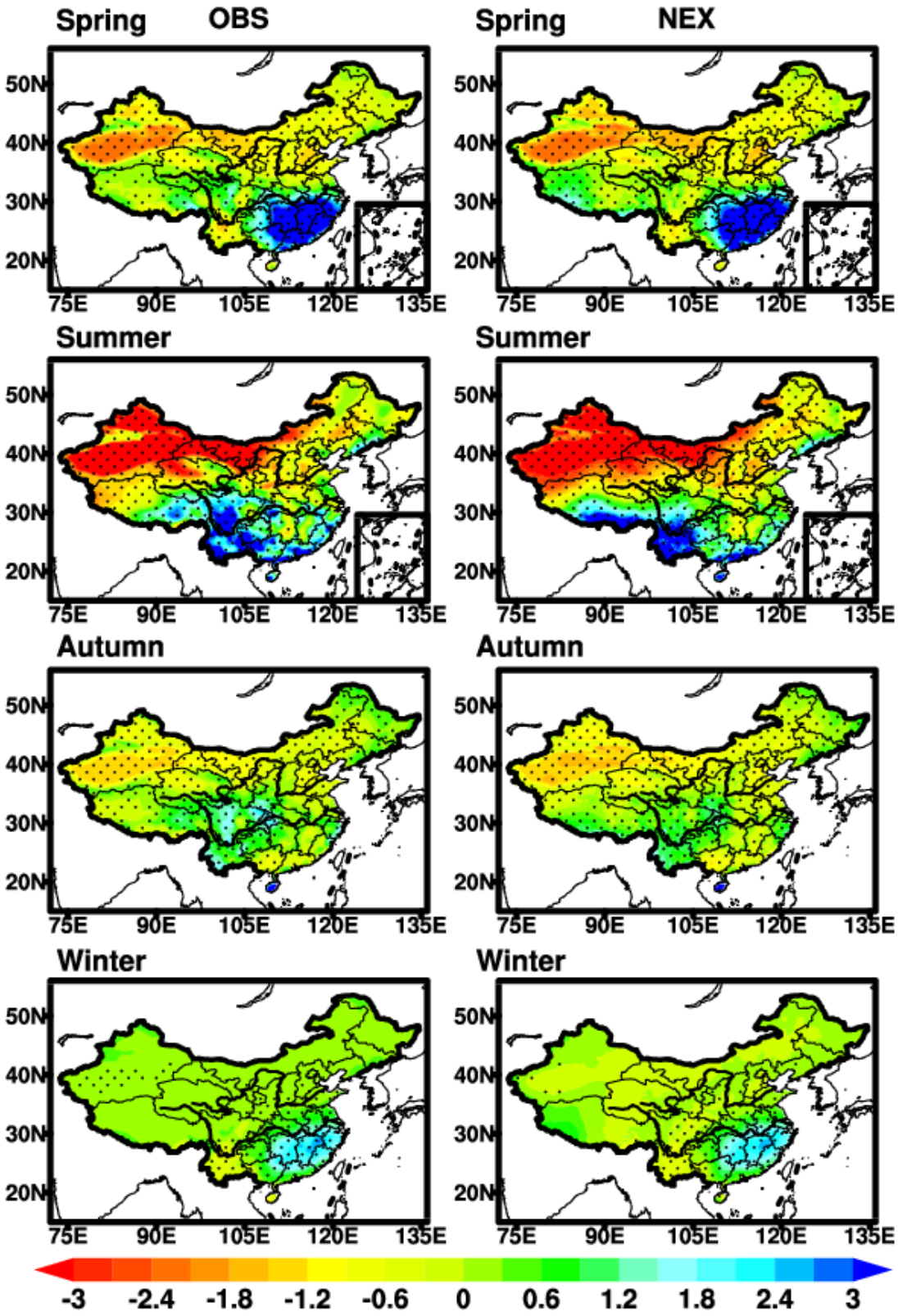

Fig 2. Comparison of mean precipitation and potential evapotranspiration (P-PET) from 1961-2005 for observation (left panel) and NEX-GDDP (right panel). Black dots indicate significant values at 95% confidence level.

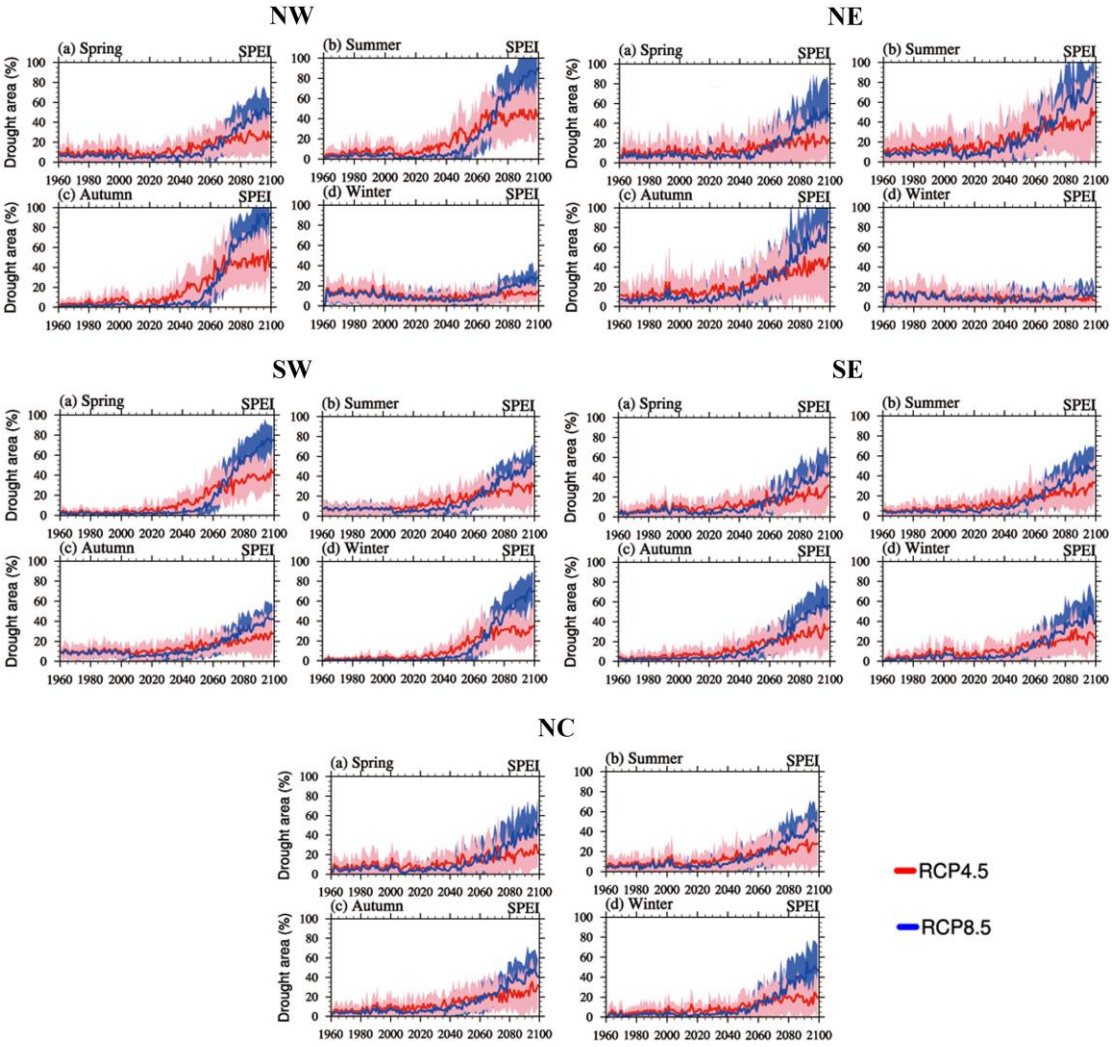

Fig 3. Spatial extent for future drought in the five subregions in China based on 3-month SPEI.

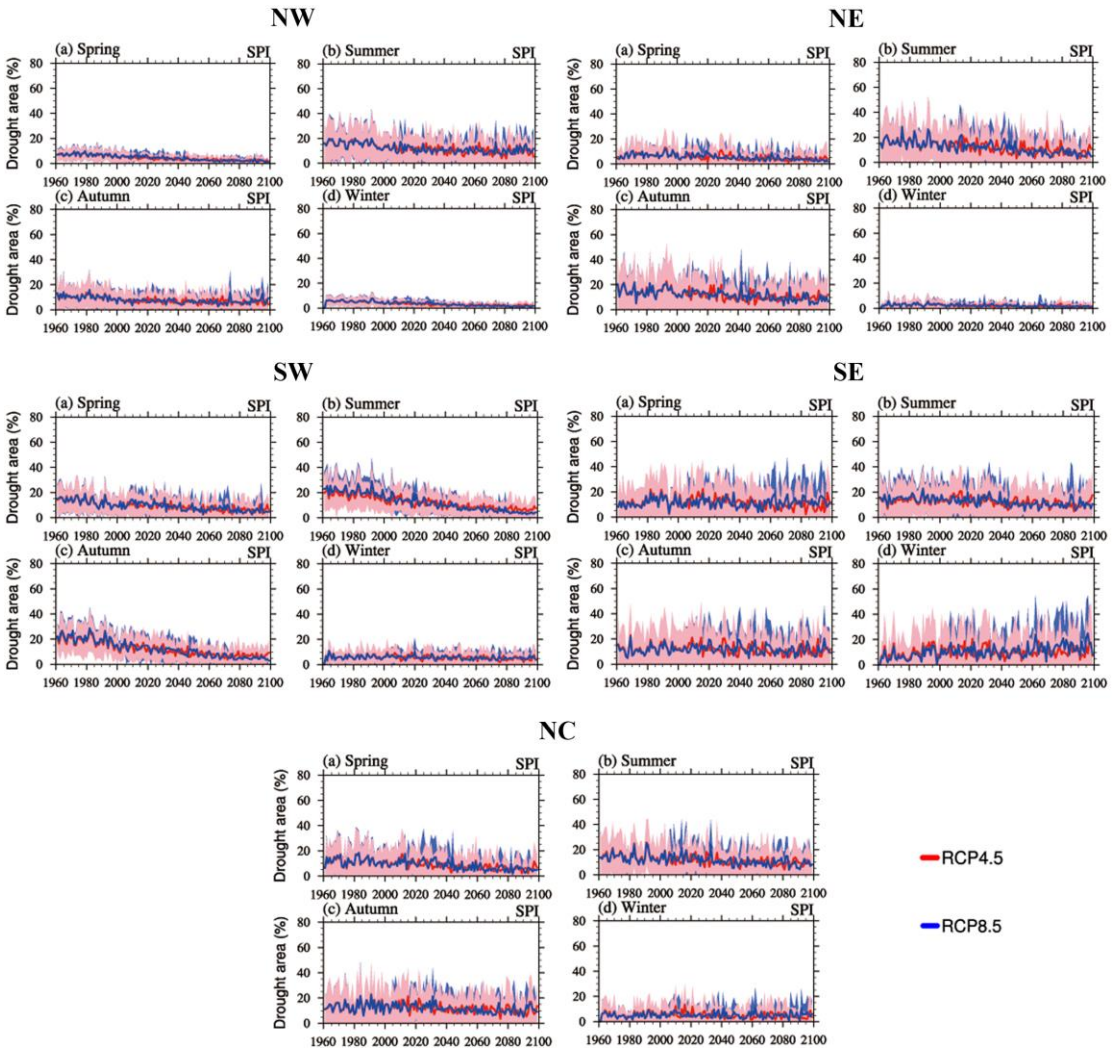

Fig 4. The same as Fig 3. But for SPI.

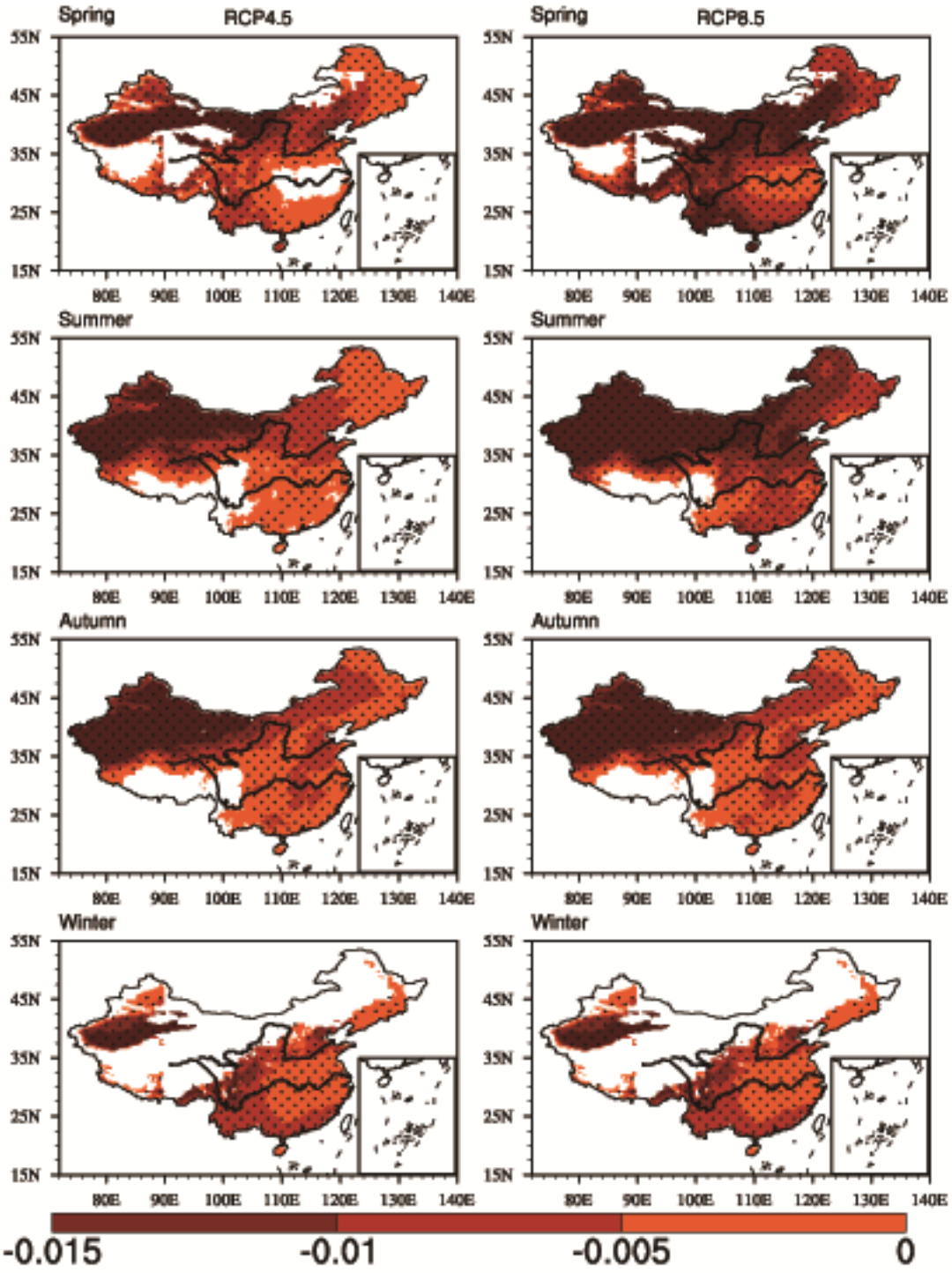

Fig 5. Long-term trends of drought during the period of 2006-2099 based on 3-month SPEI. Note that a trend with -0.01 for SPEI denotes that in 50 years, the mean value of SPEI will decrease by 0.5 (-0.01×50), this is significant for the given thresholds of -1, -1.5 and -2, which represents moderate, severe and extreme drought, respectively. Black dots indicate that trend significance exceeds the 95% confidence level.

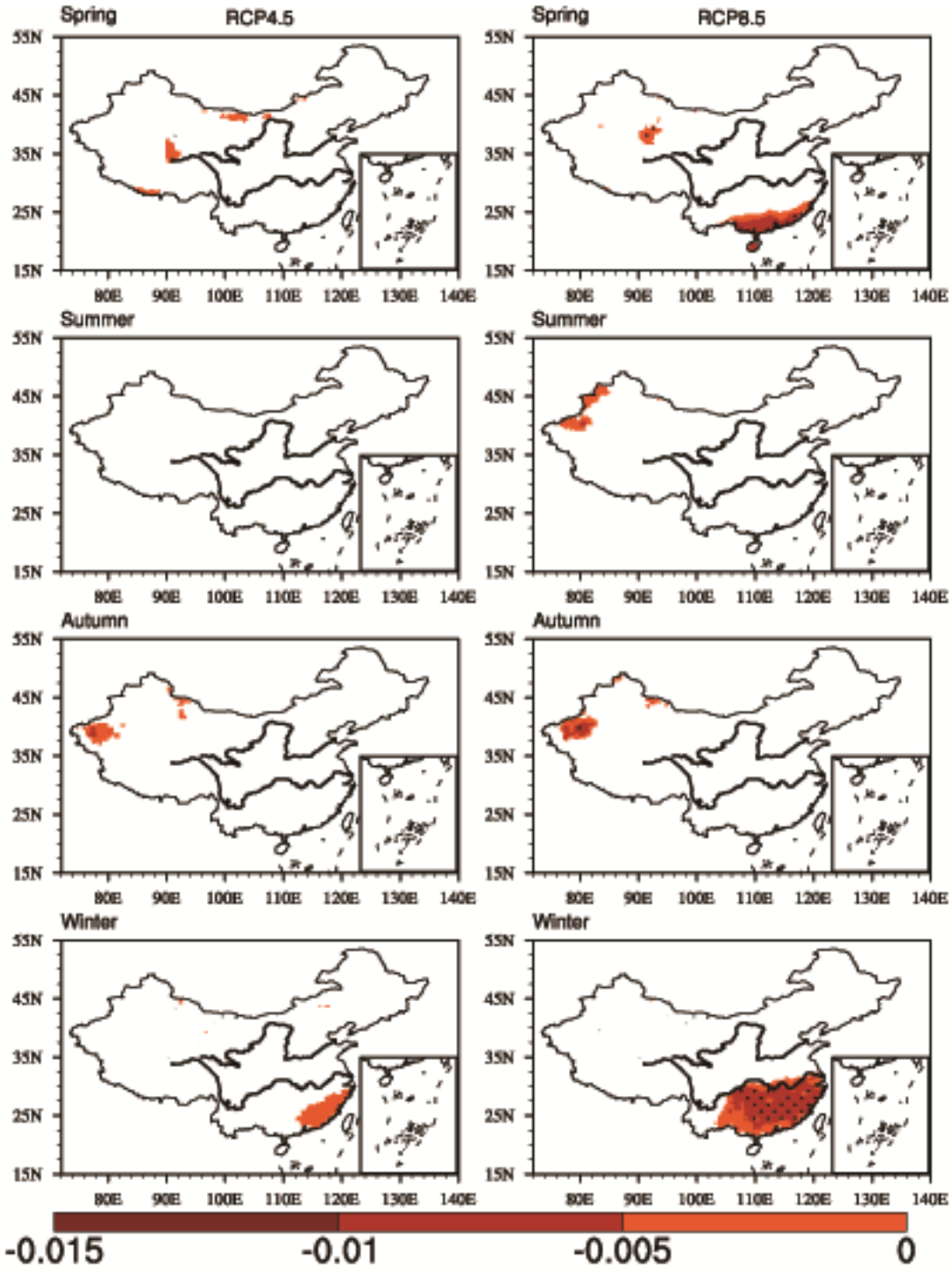

Fig 6. The same as Fig 5. But for SPI.

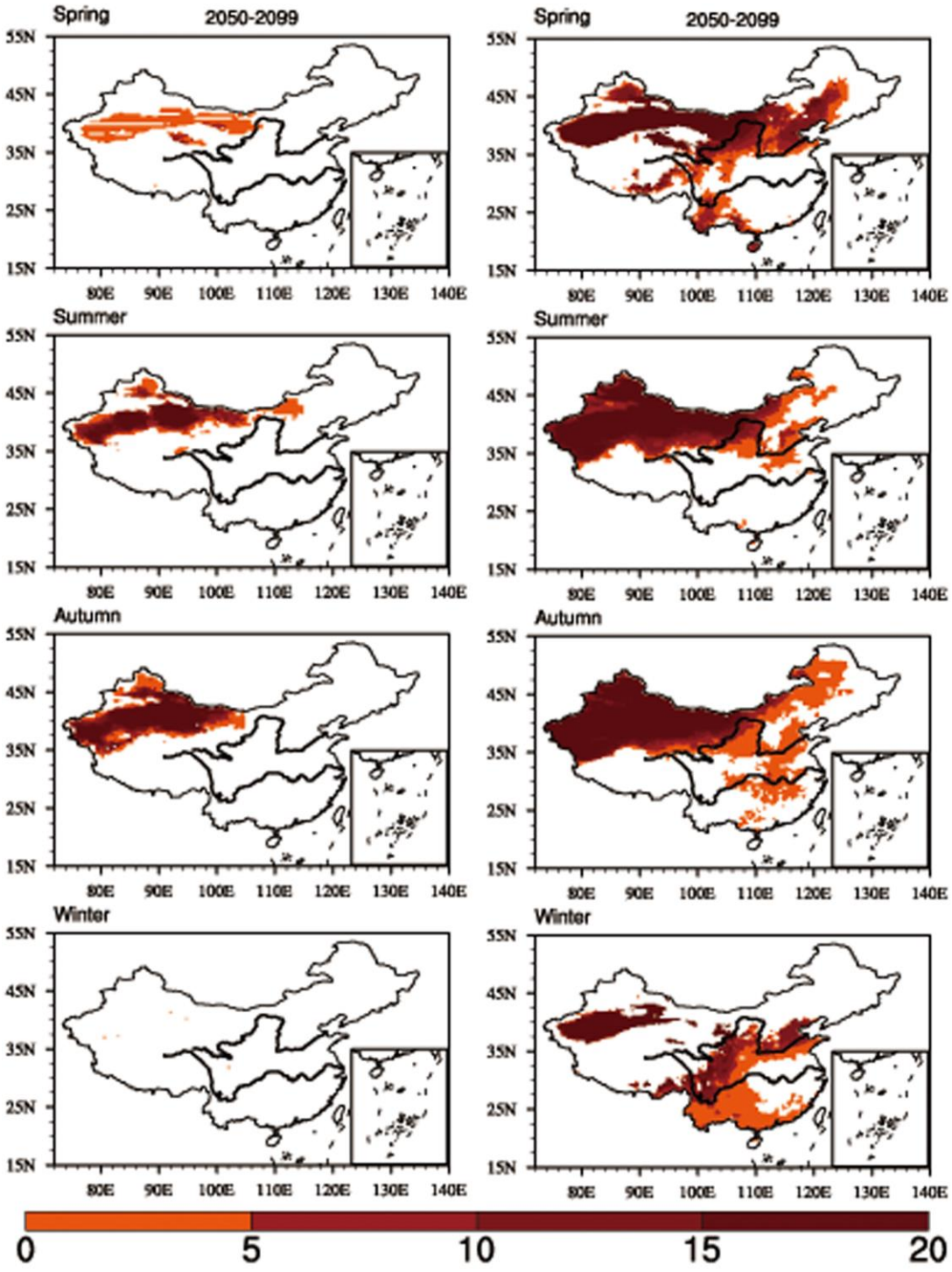

Fig 7. Changes in the number of drought events based on 3-month SPEI for RCP4.5 (left panel) and RCP8.5 (right panel).

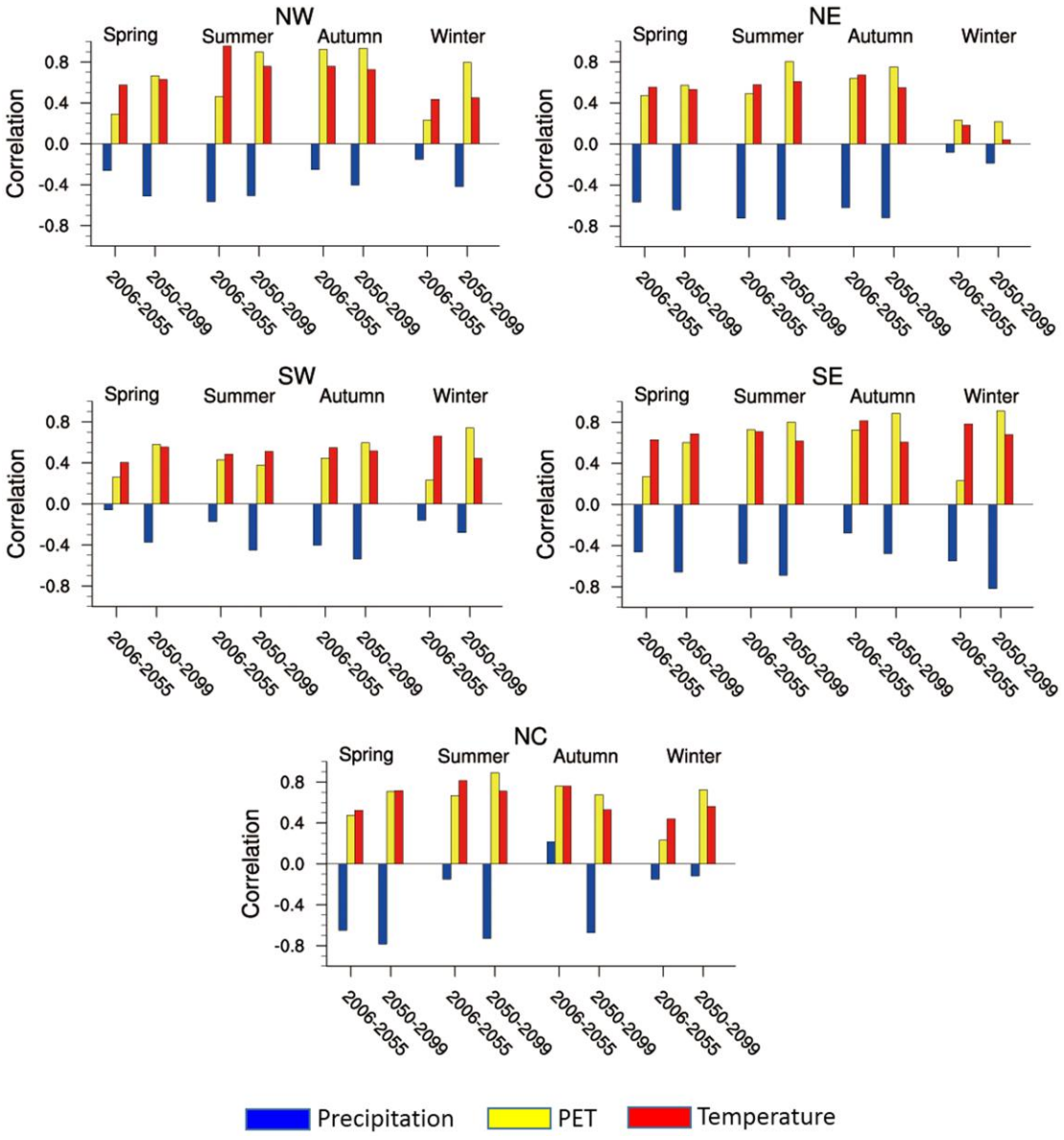

Fig 8. Spatial correlation between the variations in the number of SPEI drought events and changes in the climate variables during the 50-yr future periods for the RCP8.5 scenario.

Supporting Information for

Effect of climate change on the Centennial drought over China using High-Resolution NASA-NEX downscaled climate ensemble

Fuqiang Cao[1] and Tao Gao[2, 3, 4*]

1 School of geosciences, Shanxi Normal University, Linfen 041000, China

2 College of Urban Construction, Heze University, Heze 274000, China

3 State Key Laboratory of Numerical Modeling for Atmospheric Sciences and Geophysical Fluid Dynamics, Institute of Atmospheric Physics, Chinese Academy of Sciences, Beijing 100029, China

[4] Department of Marine, Earth and Atmospheric Sciences, North Carolina State University, Raleigh, North Carolina 27695, USA

Contents of this file

Table S1. 21 GCMs used in this study and their characteristics

No.	Model	Center	Original resolution (Lat× Lon)[a]	No. of atmospheric levels	Type
1	ACCESS1-0	Commonwealth Scientifc and Industrial Research Organization/Bureau of Meteorology, Australia	1.875 × 1.25	38	AO
2	BCC-CSM1-1	Beijing Climate Center, China Meteorological Administration, China	2.8 × 2.8	26	ESM
3	BNU-ESM	College of Global Change and Earth System Science, Beijing Normal University, China	2.8 × 2.8	26	ESM
4	CanESM2	Canadian Centre for Climate Modeling and Analysis, Canada	2.8 × 2.8	35	ESM
5	CCSM4	National Center for Atmospheric Research, United States	1.25 × 0.94	26	AO
6	CESM1-BGC	Community Earth System Model Contributors [National Science Foundation (NSF), DOE, and NCAR]	1.4 × 1.4	26	AO
7	CNRM-CM5	National Centre for Meteorological Research, France	1.4 × 1.4	31	AO
8	CSIRO-MK3-6-0	Commonwealth Scientifc and Industrial Research Organization/Queensland Climate Change Centre of Excellence, Australia	1.8 × 1.8	18	AO
9	GFDL-CM3	NOAA/Geophysical Fluid Dynamics Laboratory, United States	2.5 × 2.0	48	AO
10	GFDL-ESM2G	NOAA/Geophysical Fluid Dynamics Laboratory, United States	2.5 × 2.0	48	ESM

11	GFDL-ESM2M	NOAA/Geophysical Fluid Dynamics Laboratory, United States	2.5 × 2.0	48	ESM
12	INMCM4	Institute for Numerical Mathematics, Russia	2 × 1.5	21	AO
13	IPSL-CM5A-LR	L'Institut Pierre-Simon Laplace, France	3.75 × 1.8	39	ChemESM
14	IPSL-CM5A-MR	L'Institut Pierre-Simon Laplace, France	2.5 × 1.25	39	ChemESM
15	MIROC-ESM	Japan Agency for Marine-Earth Science and Technology, Atmosphere and Ocean Research Institute (The University of Tokyo), and National Institute for Environmental Studies	2.8 × 2.8	80	ESM
16	MIROC-ESM-CHEM	Japan Agency for Marine-Earth Science and Technology, Atmosphere and Ocean Research Institute (The University of Tokyo), and National Institute for Environmental Studies	2.8 × 2.8	80	ChemESM
17	MIROC5	Atmosphere and Ocean Research Institute (The University of Tokyo), National Institute for Environmental Studies, and Japan Agency for Marine-Earth Science and Technology, Japan	1.4 × 1.4	40	AO
18	MPI-ESM-LR	Max Planck Institute for Meteorology, Germany	1.9 × 1.9	47	ESM
19	MPI-ESM-MR	Max Planck Institute for Meteorology, Germany	1.9 × 1.9	95	ESM
20	MRI-CGCM3	Meteorological Research Institute, Japan	1.1 × 1.1	48	AO
21	NorESM1-M	Norwegian Climate Center, Norway	2.5 × 1.9	26	ESM

[a]All GCMs used are statistically downscaled to 0.25◦ resolution.

AO, coupled atmospheric-ocean model; ESM, Earth system model; ChemESM, atmospheric chemistry coupled with ESM models.